STUDY OF SILICON HYPERABRUPT JUNCTION

A Thesis Submitted
in partial Fulfilment of the Requirements
for the Degree of

MASTER OF TECHNOLOGY

By
ANIL K. GUPTA

to the

DEPARTMENT OF ELECTRICAL ENGINEERING

INDIAN INSTITUTE OF TECHNOLOGY KANPUR

AUGUST, 1975

CERTIFICATE

This is to certify that the thesis entitled 'A
Study of Silicon Hyperabrupt Junctions' by Anil K. Gupta
is a record of work carried out under my supervision and
has not been submitted elsewhere for a degree.

M.S. Tyagi

M.S. Tyagi
Assistant Professor
Department of Electrical Engineering
Indian Institute of Technology
Kanpur

EE-1975-M-GUP-STU

A C K N O W L E D G E M E N T S

NOMENCLATURE

$'V_B'$	Breakdown voltage
$'n'$	C-V index
$'q'$	Electronic charge
$'\epsilon'$	Permittivity of silicon
$'V'$	Voltage drop across the junction
$'x'$	Distance from the junction
$'W_B'$	Space charge width at breakdown
$'N_o'$	Cross over impurity concentration in the retrograded region
$'N_B'$	Background impurity concentration
$'L'$	Characteristic length of impurity profile in retrograded region
$'R_c'$	Ratio of $'N_B'$ to $'N_o'$.
$'C'$	Normalized capacitance of the junction
$'n_{max.}'$	Maximum value of $'n'$
$'V_n'$	Normalized voltage across the junction
$'N_{min.}'$	Lowest impurity concentration in retrograded region.

TABLE OF CONTENTS

CHAPTER I

INTRODUCTION

To the vast field of applications of a semiconductor
p-n junction , a significant contribution is, of its voltage
variable capacitance , in reverse bias condition. Some of the
major applications of a p-n junction, as a voltage variable
capacitance, are in parametric amplification, harmonic
generation, mixing, detection and voltage variable tuning.

The field of application of a p-n junction, as a
varactor (variable reactance) can be divided into two areas.
(1) where change in capacitance of the p-n junction, with
   voltage is used, as in tuning.
(2) where the rate of change of capacitance is used as in
   parametric amplification.

For both the areas of applications, hyperabrupt
junctions exhibit a superior characteristic to that of other
types of p-n junctions i.e. abrupt and linearly graded junc-
tions. This is because the former is more voltage sensitive
and hence provides a larger variation of capacitance and
higher rate of change of capacitance. The higher voltage
sensitivity of capacitance in hyper-abrupt junctions is
attributed to the peculiar impurity distribution near the

junction . In view of above mentioned grouping of appli -
cations,the breakdown voltage (V_B) and C-V index (n) are the
important parameters of a varactor, as the former dominantly
determines the range of variable capacitance available and
latter, the rate of change of capacitance. Both the
parameters solely depend upon the impurity distribution on
both the sides of the junction.

A hyperabrupt junction is characterized by the
uniformly doped one side of the junction, while on the
other side, the impurity concentration decreases with distance
from the junction. Uniformly doped side is generally heavily
doped while òn the other side of the junction, commonly
known as retrograded region, the impurity distribution may
be satisfying either of the exponential,complementary error
function, gaussian function or   the power law distribution.

In one-sided hyperabrupt junctions, therefore, the
breakdown voltage and C-V index will depend upon the
impurity distribution in the retrograded region. Since the
technology, today, permits high controllability of impurity
distribution, breakdown voltage and C-V index of a hyperabrupt
junction can be pre-determined, if their relationship with
impurity distribution is established.

Several authors have discussed different aspects of
breakdown in hyperabrupt junctions [1-5]. Nathanson et.al.
[4] and M.Shinoda [5] studied avalanche breakdown in silicon
hyperabrupt junctions. Both the authors, however, in the

calculation of breakdown voltage, have assumed the ionization rates of holes and electrons [6-7] to be equal. Further measurements on silicon p-n junctions by a number of investigators, revealed that this assumption is not correct. The ionization rates of electrons were found to be higher than that of holes, in silicon p-n junctions [8-15]. The dependence of avalanche breakdown voltage on impurity distribution, in hyperabrupt junctions, therefore, needs to be re-evaluated. None is known to have discussed zener breakdown in silicon hyperabrupt junctions.

A number of authors have discussed the C-V characte - ristics of hyperabrupt junctions [16-19]. A.Shimiju [16] and M.Shinoda [17], calculated the C-V characteristics of hyperabrupt junctions assuming exponential and complementary error function impurity distributions in the retrograded region,respectively. The latter author has also discussed the temperature dependence of C-V characteristics of hyperabrupt junctions. The C-V relationships, assuming power law distribution in retrograded region has also been derived [18].

_____

C-V index (n):- The C-V index is defined as the slope of the curve ln C vs. ln V where 'C' and 'V' are the capacitance of and voltage applied across the junction. It can be expressed as,

$$n = \frac{d(\ln C)}{d(\ln V)} \qquad (1.1)$$

A comparative study of C-V characteristics of the different types of hyperabrupt junctions reveals that C-V index*(n) varies with applied voltage except in the case where the retrograded region has a power law distribution. For the junctions in which 'n' varies with voltage, 'n' is found to be first increasing, reaching a maximum and then decreasing with increasing voltage. These types of the junctions are of practical interest because they can be fabricated by most widely used diffusion techniques,. A rigorous study of dependence of 'n' on the applied voltage and parameters of impurity profile in retrograded region, is of practical importance.

The present work was started with the following objectives,

(1)   To find out the dependence of avalanche breakdown voltage (V_B) and space charge width at breakdown (W_B), on the parameters which characterize the impurity distribution in the retrograded region. Also, to find out empirical relationships, expresssing V_B and W_B as a function of the impurity distribution parameters.

(2)   To find out the dependence of C-V index on the impurity distribution in retrograded region and to establish the empirical relationships expressing n_{max}, the maximum value of C-V index ,as a function of impurity profile parameters.

* See footnote on page 3.

(3)   To fabricate silicon hyperabrupt   junctions and
to investigate how far the experimentally measured
values of 'V_B' and 'n_{max}' are in agreement with the
calculated results.

AVALANCHE BREAKDOWN IN SILICON HYPERABRUPT JUNCTION

2.1   Electric field and potential distribution in space

charge region:

The assumed impurity distribution in the hyperabrupt

junction is shown in Fig.(1).   One side of the junction

has been assumed to be very heavily doped.   On the other

side i.e. in the retrograded region, the impurity concentra-

tion has been assumed to be decreasing exponentially with

distance from the junction.   This choice of impurity

distribution in retrograded region has been made for two

reasons.   Firstly because it simplifies the calculation

of the avalanche breakdown voltage and secondly, because

the exponential distribution has been found to be a good

approximation to the tails of Gaussian and complementary

error functions, the types of distributions that are

obtained from most commonly used diffusion techniques [23].

Assuming that the impurity concentration decreases

exponentially with distance from the junction, the

expression for impurity distribution in retrograded region

can be written as,

$$N(x) = (N_O - N_B) \; e^{-x/L} + N_B \qquad\qquad (2.1)$$
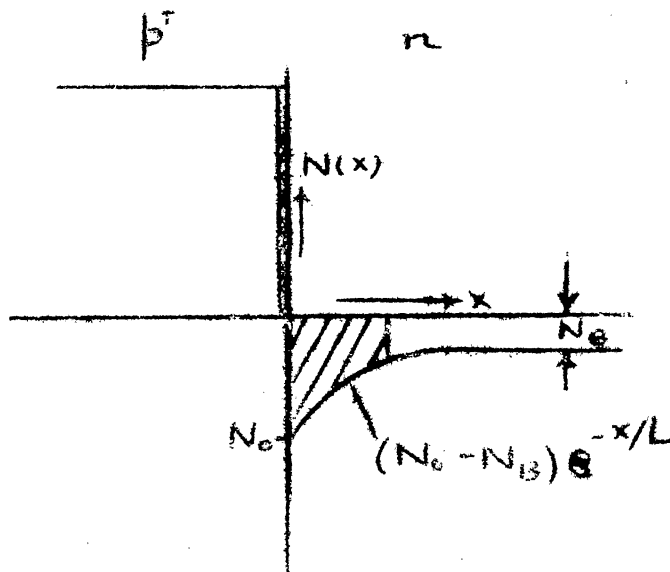
Fig. 1

where,

'x' is the distance from the junction

'N_0' is the cross over impurity concentration at the

junction, on the retrograded ~~region~~ side.

'L' is the characteristic length

'N_B' is the background impurity concentration.

Assuming that there are no mobile carriers in the space charge region and also that all the impurity atoms in the space charge region are ionized, the Poisson's equation for space charge in the retrograded region can be written as,

$$\frac{d^2V}{dx^2} = - \frac{q}{\varepsilon} \cdot N(x) \qquad (2.2)$$

Since the junction has been assumed to be very heavily doped on one side, the width of the space charge layer
is very small ᴓn this side of the junction and/potential
nearly all the

drop occurs across the space charge in retrograded region.
This yields the following boundary condition for eq. (2.2).

$$V = 0, \text{ at } x = 0 \tag{2.3a}$$

Assuming that the voltage drop across the region,
outside the space charge layer, is negligible and also that
the electric field due to inhomogeneous impurity distribution
in retrograded region is negligibly small compared to the
field in the space charge region, the second boundary
condition for eq. (2.2) can be written as,

$$E = 0 \text{ at } x = W \tag{2.3b}$$

where 'E' is electric field

and 'W' is width of space charge layer in the retrograded
region

The Integration of eq. (2.2), with the boundary
condition (2.3)b yields the equation for electric field
distribution in the space charge region.

$$-\frac{dV}{dx} = E(x) = \frac{q}{\varepsilon} \cdot N_0 \left[\left(1 - \frac{N_B}{N_0} \right) \cdot L \cdot (e^{-W/L} - e^{x/L}) + \frac{N_B}{N_0} \cdot (x-W) \right] \tag{2.4}$$

The equation for potential distribution in retrograded
region can be obtained by integrating eq. (2.4) with
boundary condition (2.3)a. The expression for potential
distribution can be given as,

$$V(x) = \frac{q}{\varepsilon} \cdot N_0 \left[(1 - \frac{N_B}{N_0}) \cdot L \cdot (L - L \cdot e^{-x/L} - W \cdot e^{-W/L}) \right.$$

$$\left. + \frac{N_B}{N_0} \cdot (x \cdot W - \frac{W^2}{2}) \right] \tag{2.5}$$

From eqs. (2.4) and (2.5) , the expressions for maximum electric field ($E_{max.}$) , which occurs at x=0 and total voltage drop across the junction, V(W), can be obtained. Thus,

$$E_{max} = E(o) = \frac{q}{\varepsilon} \cdot L \cdot N_0 \left[(1 - \frac{N_B}{N_0}) \cdot (e^{-W/L} - 1) \right.$$

$$\left. - \frac{N_B}{N_c} \cdot \frac{W}{L} \right] \tag{2.6}$$

and

$$V(W) = V_a + V_D = \frac{q}{\varepsilon} \cdot L^2 \cdot N_0 \left[(1 - \frac{N_B}{N_0}) (1 - (1 - \frac{W}{L}) e^{-W/L}) \right.$$

$$\left. - \frac{N_B}{N_0} \cdot \frac{W^2}{2L^2} \right] \tag{2.7}$$

where,

V_a = voltage applied across the junction

V_D = Built in potential of the junction.

2.2   Avalanche breakdown in a hyperabrupt junction:

The threshold condition for avalance breakdown in a p^+-n junction, where avalanche multiplication is initiated by holes, is given by [20],

$$\int_0^{W_B} \alpha_p \cdot \exp \left[-\int_0^x (\alpha_p - \alpha_n) \, dx' \right] dx = 1 \tag{2.8}$$

and the same for an n^+-p junction where avalanceh multipli-

cation is initiated by electrons is given by [20].

$$\int_0^{W_B} \alpha_n \cdot \exp \left[-\int_0^x (\alpha_n - \alpha_p) \, dx' \right] \cdot dx = 1 \qquad (2.9)$$

where,

'W_B' is the space charge width in retrograded region
at breakdown

'α_p' and 'α_n' are the ionization rates of holes and
electrons, respectively.

In the eqs. (2.8) and (2.9), the space charge width in the
heavily doped region has been assumed to be negligible.

All the experimental results have shown that electric
field dependence of ionization rates can be expressed by
[9-10]

$$\alpha(E) = a \cdot \exp \left[-(b/E)^m \right] \qquad (2.10)$$

where 'E' is electric field and 'a, b, m are constants. One of
the early reliable estimates of a, b and m was made by Sze
and Gibbons [20] from the results of Lee et.at [8]. More
recent experiments of Van Overstraeten and De Man [13] on
silicon p-n junctions and of Wood et. at [14] on silicon
Schottky barriers have resulted in ionization rates different
from those obtained by Lee et.at [8]. In spite of this
difference, it is interesting to note, that the breakdown
voltages calculated from these different values of ionization
rates do not differ from each other to any great extent and

are in good agreement with the experimentally measured
values , both in abrupt as well as linearly graded junctions
[15]. We have used the values of a,b and m given by Sze
and Gibbons [20]. The values of a and b for electrons, in
silicon, are 3.80×10^6 cm^{-1} and 1.75×10^6 V/cm. respectively and
the same for holes are 2.25×10^7 cm^{-1} and 3.26×10^6 V/cm.,
respectively. m is unity for both, the holes and electrons.

It has been found [29] that for the same limits of
integration, the breakdown field for p^+-n junction is slightly
higher than that for n^+-p junction. However, because p^+-n
junctions are invariably used in hyperabrupt varactors ~~junctions~~ and
also because the difference is not very significant, the
breakdown voltage calculations have been done only for
p^+-n junctions. The eq. (2.8) has been solved numerically
for W_B, by Simpson's rule. The sequence of calculation is
as follows.

'W_B' is first given an initial value 'W' which is less
than the expected value of 'W_B'. This initial value has been
selected to be equal to the space charge width at breakdown
of a one sided abrupt junction, with impurity concentration
on lightly doped side equal to 'N_0'. 'W' is now increased
in small steps, till 'W' reaches 'W_B' the value at which
ionization integral becomes unity.

To determine 'W_B' accurately, the number of subintervals,
into which the range of integration ($0-W_B$) has been divided,
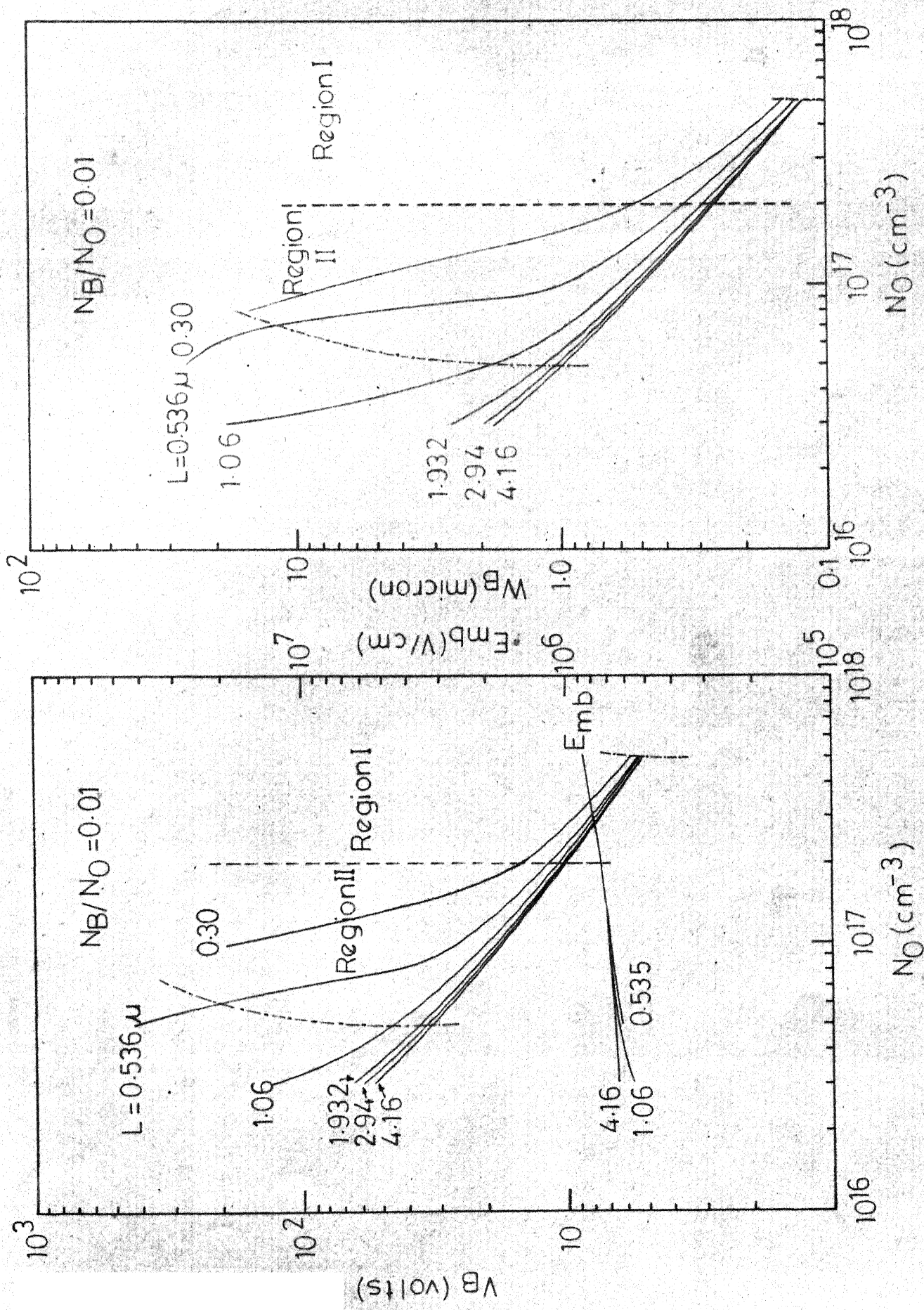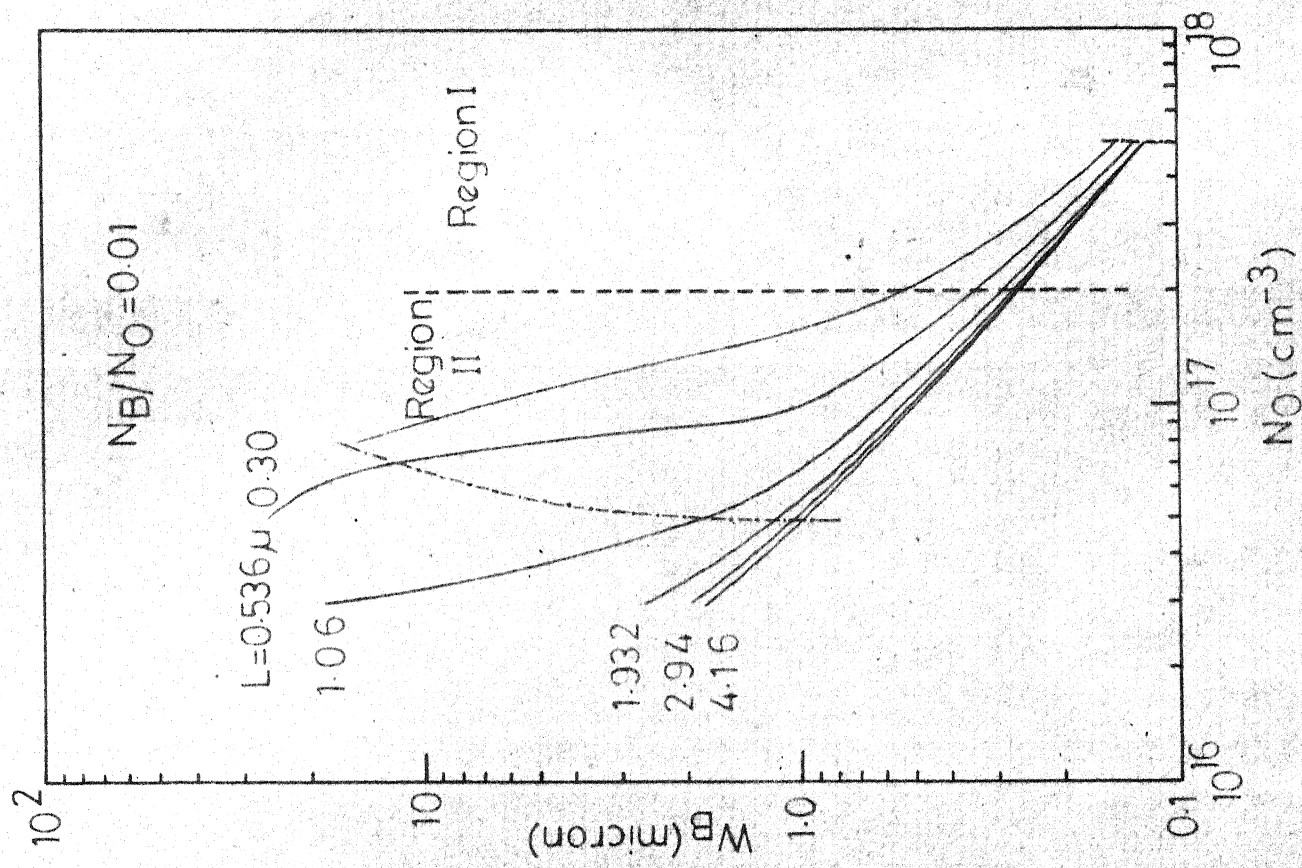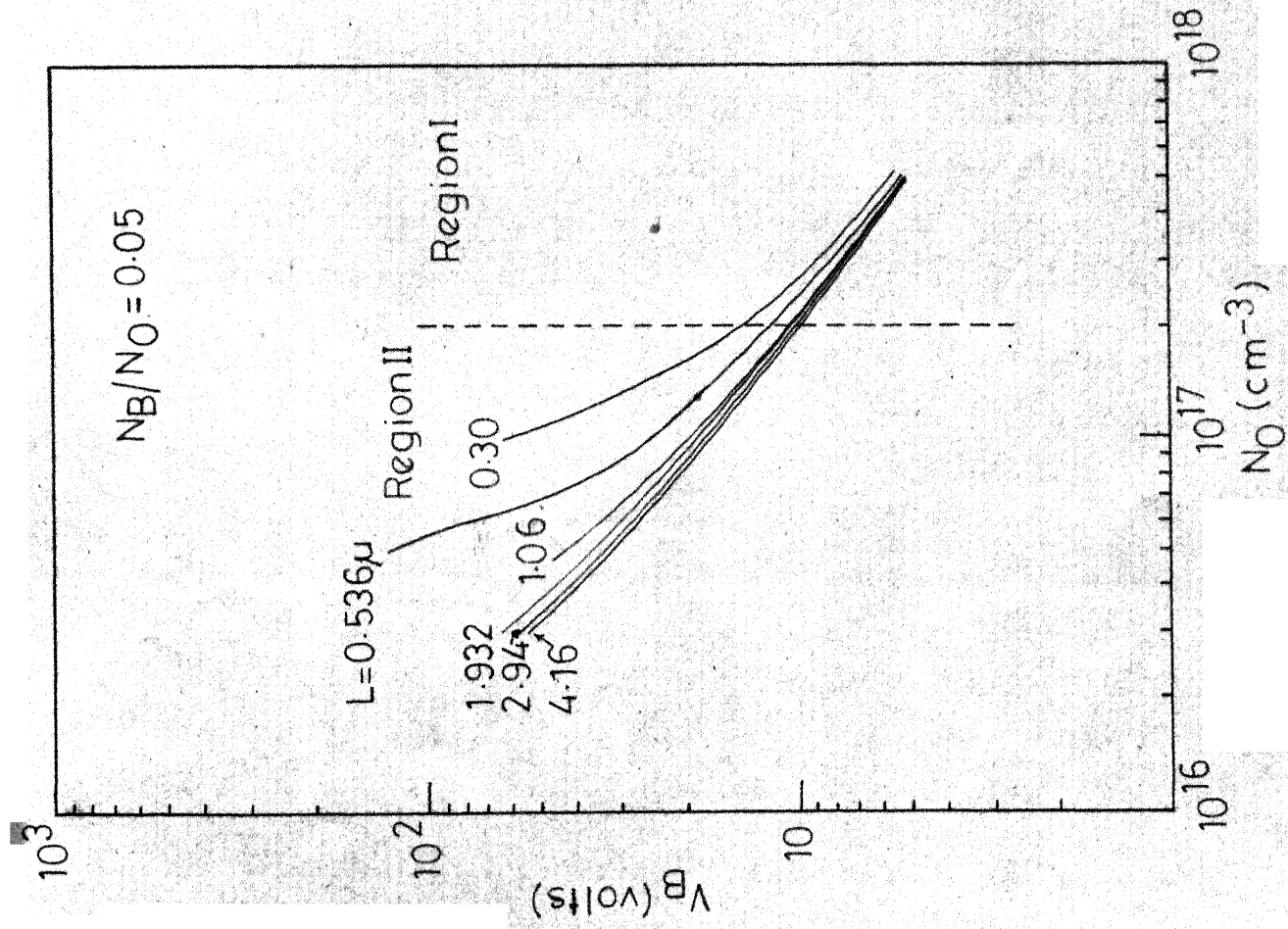is increased in steps till the increment in the number of
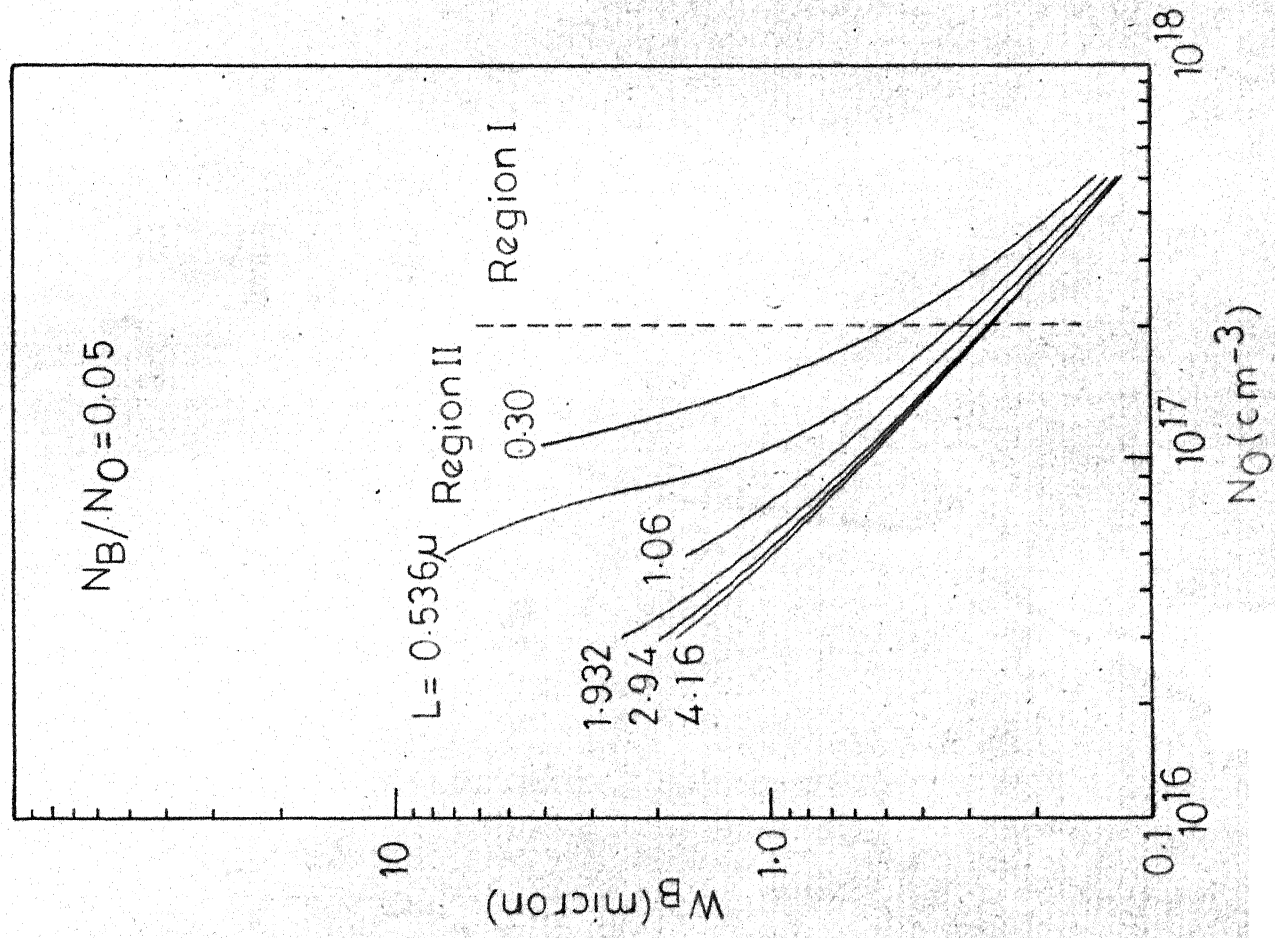
Fig. 2(a).

Fig. 2 (b).

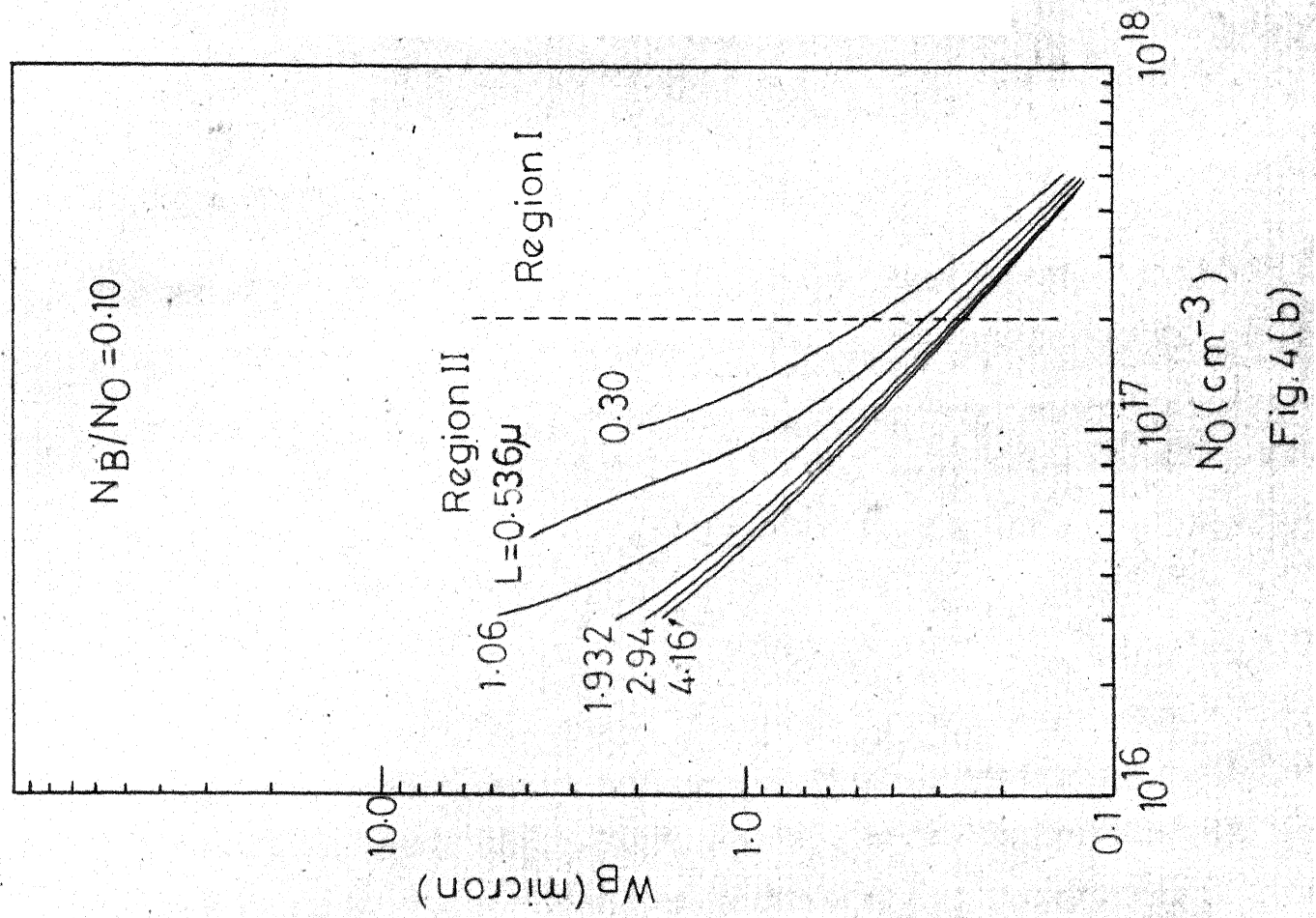Fig.3(a)

Fig.3(b)

Fig.4(a)

Fig.4(b)
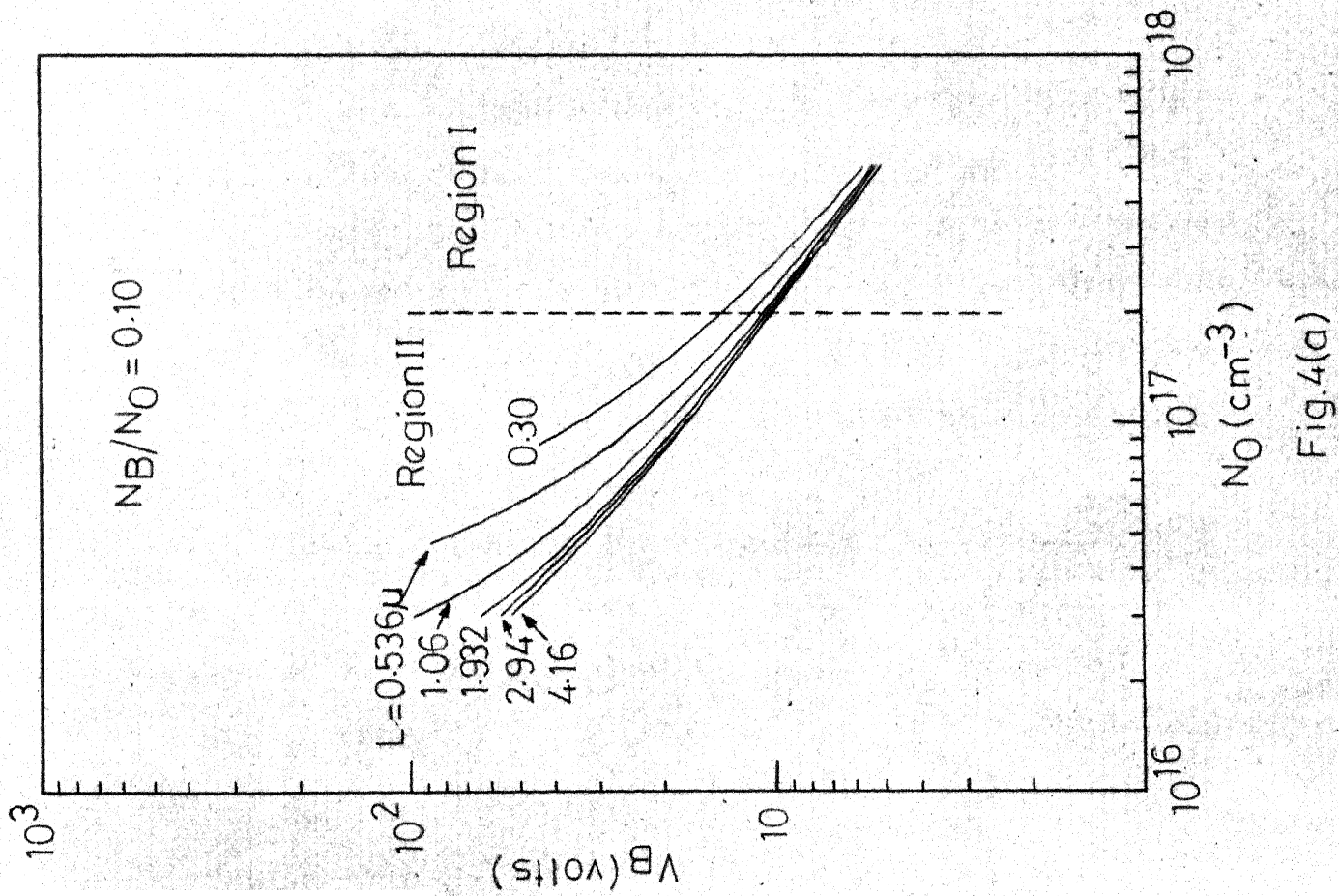
subintervals ceases to cause a change in $\bar{W_B'}$. It is relevent
to point out that the ranges $0-W_B$ and $0-x$ have been divided
into equal number of subintervals.

To obtain the breakdown voltage (V_B) and maximum
electric field at breakdown (E_{mb}) , $'W_B'$ has been substituted
for $'W'$ in equations (2.7) and (2.6) respectively.

These calculations for $'V_B'$ and $'W_B'$ have been made for
a number of values of $'N_o'$ in the range 3×10^{16} cm^{-3} to
5×10^{17} cm^{-3}., with $'L'$ given different values in the range
0.3 micron to 4.16 miron and $\frac{N_B}{N_o}$ given the values 0.1, 0.05
and 0.01, respectively. $'V_B', 'W_B'$ and $'E_{mb}'$ have been plotted as
function of $'N_o'$, with $'L'$ as parameter, for the different
values of N_B/N_o [Fig. (2),(3) and (4)].

It can be seen that $'V_B'$ and $'W_B'$ very strongly depend
upon $'N_o'$ [Fig. (2),(3) and (4)]. $'L'$ is seen to affect $'V_B'$
and $'W_B'$, only for lower values of $'N_o'$ and $'L'$. Also, a
comparison of Fig. (2) with Fig. (3) and Fig. (4) reveals that
N_B/N_o affects $'V_B'$ and $'W_B'$ only for values of $'L'$ below 1.06
micron . The nature of these curves can be explained as
follows.

For the sake of convenience the $\bar{V_B'}$ versus $'N_o'$ and $'W_B'$
versus $'N_o'$ plots have been divided into two regions, on the
basis of value of $'N_o'$. The region I is that part of the
plots where $'N_o' \geq 2 \times 10^{17}$ cm^{-3} and the part of the plots,
where $'N_o' < 2 \times 10^{17}$ cm^{-3} is depicted as region II.

In region I, for values of 'L' greater than 1.06 micron it can be seen that W_B is very small compared to 'L'. In such a case, the impurity concentration at x=0 is not very different from that at $x=W_B$ and the junction behaves more or less like an abrupt junction, with impurity concentration on lightly doped side equal to N_0. The calculated breakdown voltages in these cases are nearly same as that of the abrupt junctions.

For those cases in the region I, where $L \leqslant 1.06$ micron and in region II where $L > 1.06$ micron , it can be seen that the ratio W_B/L is much larger than that mentioned in the last paragraph. The voltage V_B and space charge width W_B for such junctions are significantly greater than those for abrupt junction with effective impurity concentration equal to N_0. These are the cases where hyperabrupt nature of the junction significantly shows up.

In region II for $L \leqslant 1.06$ micron , the effect of 'L' and N_B/N_0 on V_B and W_B shows up prominantly. In these cases, the space charge has covered the major part of the retrograded region, before breakdown occurs . It is seen that V_B and W_B are very sensitive to variations in 'L' and N_B/N_0, in this part of region II.

The maximum electric field(E_{mb}) has been plotted against N_0, for different values of 'L' in Fig. (2)a. Because E_{mb} has been found to be more or less constant with variations in N_B/N_0, it has not been found necessary to

plot it for remaining values of N_B/N_o. 'E_{mb}' , as expected, is found to be maximum for $N_o = 5 \times 10^{17}$ cm^{-3} and is equal to 8.64×10^5 V/cm. Since tunneling current in silicon p-n junctions is significant only at electric fields higher than 10^6V/cm.[21], the mechanism of breakdown in all the cases considered above,can safely be assumed to be the avalanche breakdown.

2.3   Zener breakdown in hyper-abrupt junctions:

As can be seen from Fig. (2)a, the highest value of 'E_{mb}' corresponds to low breakdown voltages (Region I, L 1.06 micron) . As explained earlier the hyperabrupt junction, in these cases, behaves more or less like an abrupt junction. The zener breakdown which occurs at very high electric fields ($> 10^6$V/cm.), can be expected to occur only in the junctions in which $N_o > 5 \times 10^{17}$ cm^{-3}, and 'L' is also larger than 1.06 micron , so that the space charge width is low enough to provide high electric field required for the tunneling of electrons. Such junctions, however, are sure to behave like an abrupt junction. For this reason, it has not been necessary to discuss the zener breakdown in hyperabrupt junctions.

2.4   Empirical relationship between 'V_B','W_B' and 'N_o','L','N_B':

By linear regression method [22], it has been found that 'V_B' and 'W_B' can be approximately expressed as a function of 'N_o','L,' and 'N_B', by the following empirical relations.

$$\ln (V_B) = 6.92 - 0.85 \ln (N_{on}) - 0.113 \ln (L) - 0.29 \ln \left(\frac{N_B}{N_o}\right)$$
$$(0.08) \quad (0.014) \qquad (0.016) \qquad (0.043)$$

$$-0.05 \ln (N_{on}) \tag{2.11}$$
$$(0.04)$$

For the above equation $R^2 = 0.973, \bar{R}^2 = 0.972$

and,

$$\ln(W_B) = 4.63 - 1.075 \ln (N_{on}) - 0.28 \ln(L)$$
$$(0.13) \quad (0.025) \qquad (0.026)$$

$$- 0.008 (N_{Bn})^{-2}$$
$$(0.023) \tag{2.12}$$

For equation (2.12), $R^2 = 0.941$, $\bar{R}^2 = 0.939$

where,

$$N_{on} \quad = \quad N_o/10^{15}$$

$$N_{Bn} \quad = \quad N \, N_B/10^{15}$$

L and W_B are in microns

V_B is in volts

Equations (2.11) and (2.12) do not hold good in the region outside the region bounded by the chain lines in Fig.(2)a and Fig.(2)b. Also the last two terms of the equation (2.11) are zero for the cases in which N_o 10^{17}cm^{-3}. The quantities written below the co-efficients, in brackets, are standard errors of respective co-effecients. For difinition of R^2 and $\bar{R}^2$ see appendix.

CHAPTER III

C-V CHARACTERISTICS OF HYPERABRUPT JUNCTIONS

3.1   Derivation of the C-V characteristic:

The C-V characteristic of the hyperabrupt junction can be derived from eqn. (2.7). of the last chapter which is again written below,

$$V(W) = V_a + V_D = \frac{q}{\varepsilon} \cdot N_o \cdot L^2 \left[\left(1 - \left(1 + \frac{W}{L}\right) e^{-W/L}\right) \right.$$

$$\left. \cdot \left(1 - \frac{N_B}{N_o}\right) + \frac{N_B}{N_o} \cdot \frac{W^2}{2L^2} \right] \tag{3.1}$$

This equation can be written in the following form.

$$V(W) = V_o \left[(1-R_c) \cdot \left(1 - (1 + 1/C) e^{-1/C}\right) + \frac{R_c}{2 C^2} \right] \tag{3.2}$$

where,

'R_c' is equal to N_B/N_o

'C' is the normalized capacitance and is equal to L/W.

'V_c' is equal to $q \dfrac{N_o L^2}{\varepsilon}$

A dimensional analysis of different terms of the eq. (3.2) reveals that 'R_c' and 'C' are dimensionless quantities while 'V_o' has the dimensions of voltage. Since

V_o' is constant for a junction, it can be used as a normalizing factor for $V(W)$. The eq. (3.2) therefore, can be further written as,

$$V_n = (1-R_c)\left(1-(1+\frac{1}{C})\,e^{-1/C}\right) + \frac{R_c}{2C^2} \qquad (3.3)$$

where $V_n = \dfrac{V(W)}{V_o}$ is the normalized voltage.

3.2   Dependence of C-V index (21) upon impurity profile
        parameters of retrograded region:

The equation for C-V index can be derived from the C-V relationship of hyperabrupt junction i.e. eq. (3.3). Differentiating both the sides of eq. (3.3), with respect to 'C' one obtains,

$$\frac{dV_n}{dC} = -\frac{(1-R_c)e^{-1/C} + R_c}{C^3} \qquad (3.4)$$

Hence,

$$n = \frac{d(\ln C)}{d(\ln V_n)} = -\,C \,\frac{C^2\left[(1-R_c)\left(1-(1+1/C)e^{-1/C}\right)+\frac{R_c}{2C^2}\right]}{(1-R_c)\,e^{-1/C} + R_c} \qquad (3.5)$$

The minus sign on right hand side indicates that the plot of $\ln C$ versus $\ln V_n$ has a negative slope. Equation (3.5) also shows that n can be expressed as a function of two variables, 'C' and 'R_c'. 'V_n' and 'n' have been calculated for different values of 'C' and 'R_c' using eqs. (3.3) and (3.5) respectively. 'n' has been plotted as a function of 'C'
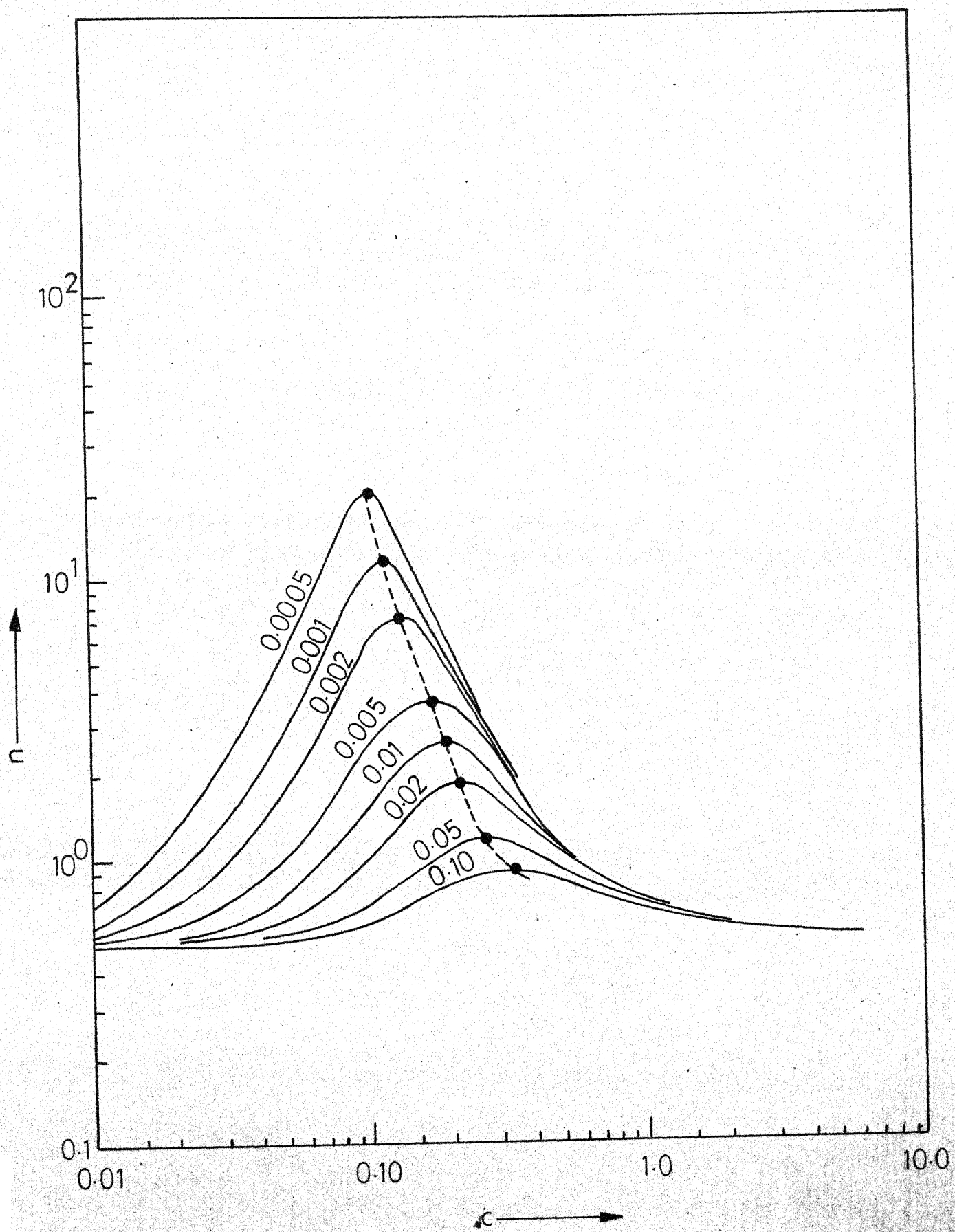
Fig. 5.

and 'V_n' in Figs. (5)and (6) respectively with 'R_c' as parameter.

It is seen from Fig. 5 that for a given value of 'R_c', 'n' first increases reaches a maximum and then starts decreasing with increasing 'C' [Fig. (5)]. For very low as well as for large values of 'C', 'n' is seen to approach the value 0.5, which is the C-V index of an abrupt junction. The dotted curve is the plot of n_{max}. as a function of 'C'. The nature of the n versus 'C' curves of Fig. 5 can be explained as follows.

For large values of 'C' i.e. low values of 'W', the space charge is confined to the region near the junction, where impurity concentration is very high. In this situation, the change ΔW in 'W' caused by a differential increase ΔV in 'V' is very low. The impurity concentration at x =W and at x = W + ΔW, therefore, are almost equal and junction behaves more or less like an abrupt junction . As the space charge moves further in the retrograded region, the impurity concentration decreases and same amount of change in voltage causes higher and higher change in 'W', thereby increasing the value of 'n' . At very low values of 'C' or far away to the left of the maximum points where the space charge has covered practically whole of the retrograded region and has entered the substrate region, the junction again exhibits abrupt

junction characteristics, because the impurity concentration in substrate region does not change with the distance.

A careful inspection of GFig. (5) also reveals that maximum value of n, $n_{max.}$' depends on 'R_c' only. A plot of $n_{max.}$, as a function of R_c is shown in Fig. (6). It is seen that '$n_{max.}$' increases with decreasing 'R_c'. This is expected because as R_c increases and approaches unity the junction tends to become an abrupt junction.

C-V index (n) has also been plotted as a function of 'V' [Fig. (7)]. It is interesting to note that 'n' is always maximum when 'V' is approximately unity.

3.3   Relationships between'$n_{max.}$' 'R_c' and 'C':

Empirical relationship expressing 'C' as a function of '$n_{max.}$' and 'n_{max}' as a function of R_c have been eobtained by linear regression method [22]. Former relationship is given as,

$$\ln(10C) = 4.43 + 0.39\ln (10\, n_{max.}) - 2.8 \sqrt{\ln (10\, n_{max.})} \qquad (3.6)$$
$$(1.07)\ \ (0.3) \qquad\qquad (1.15)$$

For the equation, $R^2 = 0.986$ and $\bar{R}^2 = 0.98$

The latter relationship is, as given below,

$$\ln (10^4 n_{max.}) = 7.98 - 0.68 \ln (10\, R_c) + 5.29 \exp (R_c) \qquad (3.7)$$
$$(0.61)\ \ (0.012) \qquad\qquad (0.64)$$

The values of R^2 and $\bar{R}^2$ for this eq. are, $R^2 = 0.999$ and $\bar{R}^2 = 0.999$.

The quantities written below the coefficients, in brackets, are standard errors of respective co-efficients.
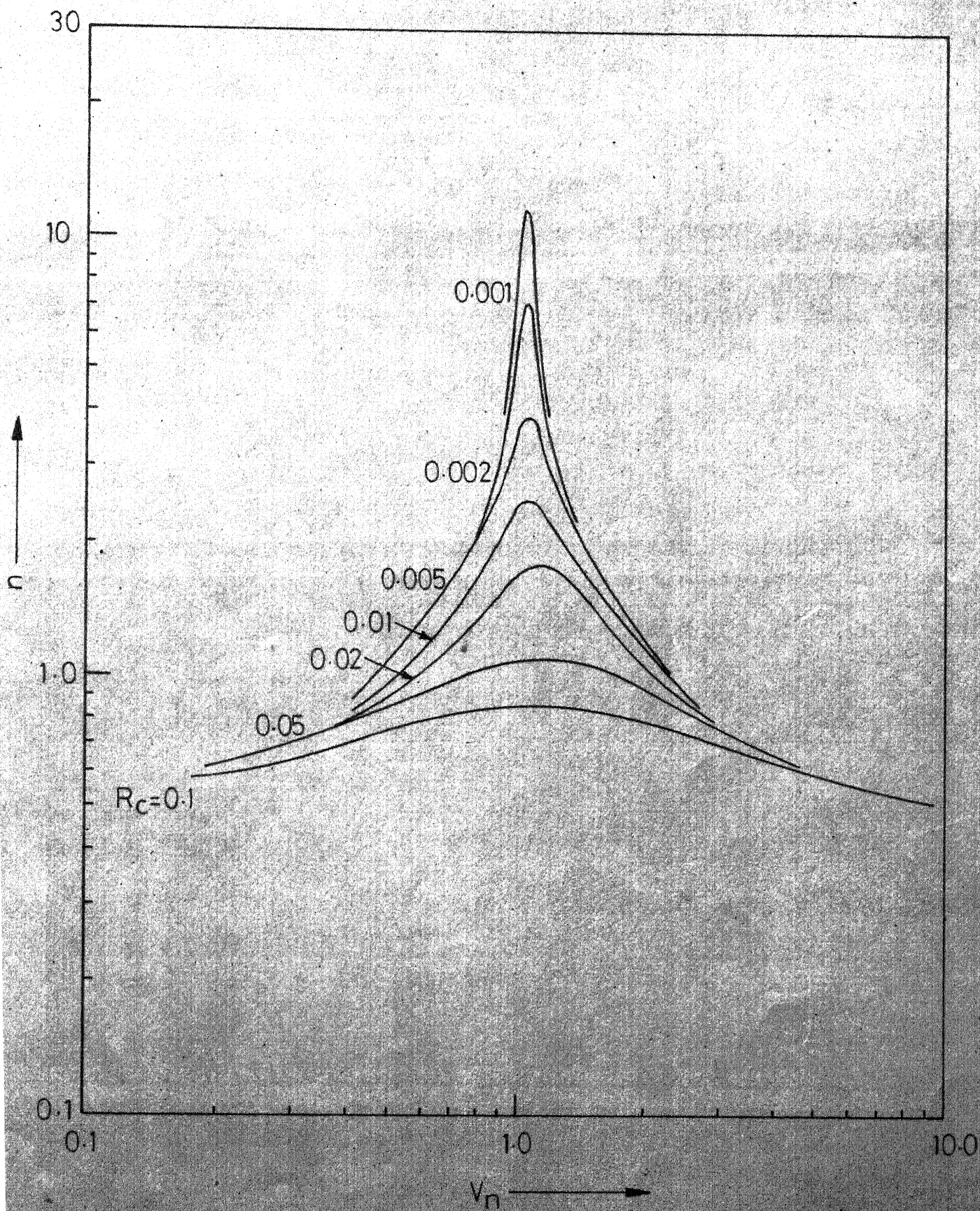
Fig. 6.

The interpretation of R^2 and $\bar{R}^2$ has been given in appendix.

The above expressions as well as the empirical expression given in Chapter II have been obtained by using a standard regression program available in Computer Centre Library, I.I.T. Kanpur.

Fig.7.

R_c

n_{max}
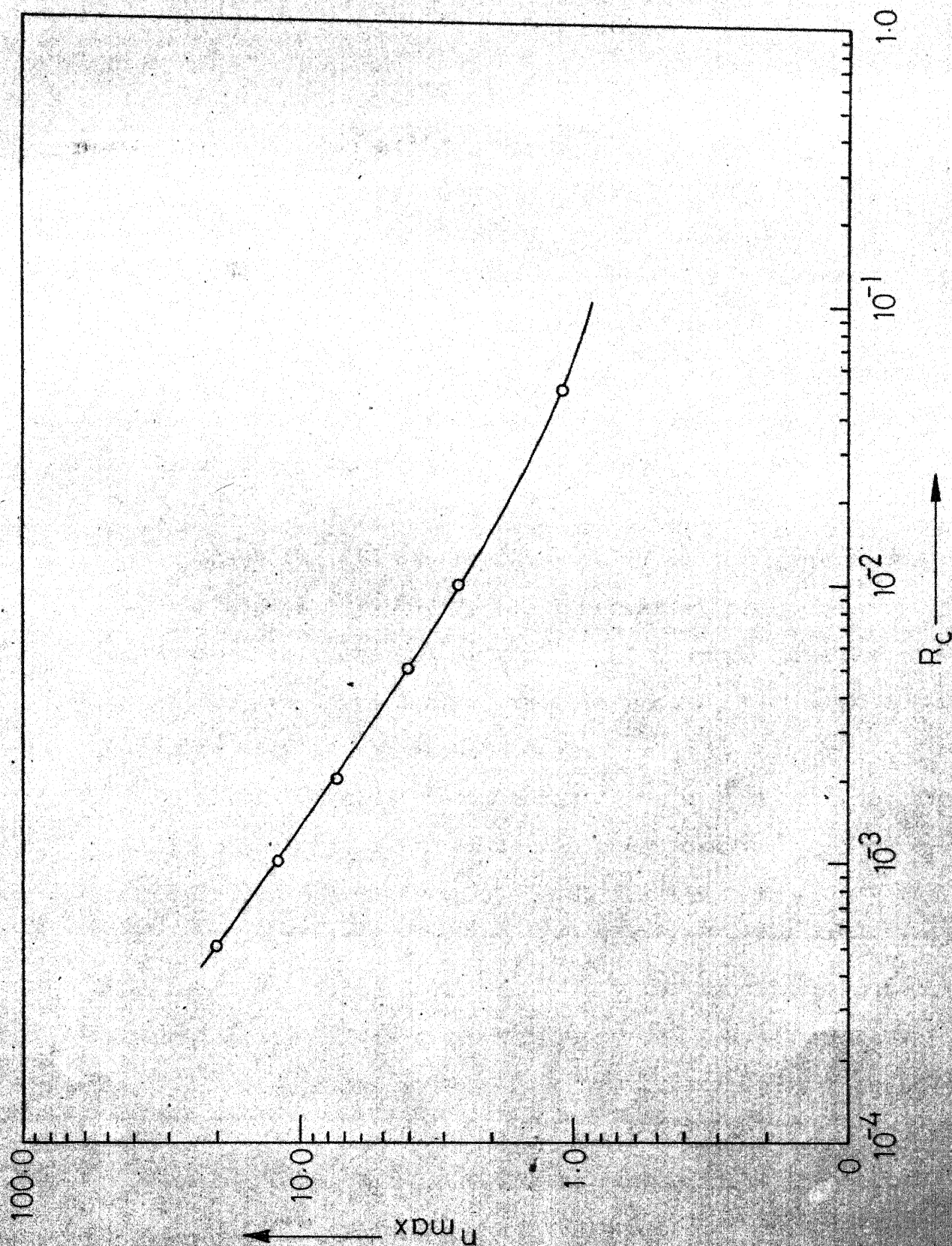
CHAPTER IV

EXPERIMENTAL WORK

4.1   Fabrication Technology:

Several techniques have been reported for fabricating the hyperabrupt junctions. Major among them are (i) alloy diffusion [1-4] (ii) double diffusion [24] (iii)epitaxial growth [25] and (iv) ion implantation [26]. In our work the double diffusion process has been used.

4.1.1 Design Considerations:

Since the aim of the fabrication of the hyperabrupt junction has been to verify the theoretically calculated results the device structure and the values of impurity profile parameters are to be decided from the point of view of verification of theoretical results only.

The fabricated junction has to be a p^+-n type, because all the calculations for avalanche breakdown voltages have been made for p^+-n junctions only. Also for the measurement of true breakdown voltage of the junction, it is necessary that the structure of the device is mesa type, as this structure eliminates the effect of curvature of the junction (curvature lowers the breakdown voltage) on the breakdown voltage [27].

Further as explained in Chapter II , the junctions with N_o 2×10^{17} and L   1.06 micron, behave like the abrupt junctions. The fabrication of the junctions having 'N_o' and 'L'

in this range, therefore, can be dispensed with.

4.1.2 Fabrication Process:

The hyperabrupt p^+-n junctions were fabricated on n-type silicon wafers, polished on one side. The resistivity of the wafers was specified to be in the range 3-7 ohms.cm. and the measured thickness was 8 mils. The complete process of fabrication comprises of following steps.

Step I Cleaning:

After degreasing, the wafer was cleaned by boiling it in the sulnit solution (Conc. H_2SO_4 + Conc. HNO_3, 1: 1 by volume) for 10 minutes. A thorough rinsing in distilled de-ionized water (DDIW) and drying in hot air followed the cleaning in sulnit solution. The wafer was then transferred to the phosphorous diffusion system.

Step II Phosphorous Diffusion:

A liquid dopant $POCl_3$ was used as source for phosphorous diffusion. Deposition was done at $800^\circ C$, for 10 minutes. The flow rates of oxygen, source nitorgen (used to bubble the $POCl_3$) and carrier nitrogen were maintained at 40 c.c./min., 15 c.c./min. and 350 cc /min. respectively. This was followed by a drive -in at $1100^\circ C$ for 2 hours. The calculated surface concentration and diffusion length $(L_d)^*$ under these diffusion conditions are 7.9×10^{18} cm^{-3} and 1.06 micron respectively.

Step III Formation of Exponentially Retrograded Region:

Since the impurity distribution expected from the above described diffusion is Gaussian function , only the tail of

* See footnote on page 23.

which (about two decades below the surface concentration) can be closely approximated to the exponential profile, it was considered necessary to etch out a small thickness of wafer so as to expose the surface where the impurity concentration of original Gaussian distribution has fallen by two orders of magnitude . This etching also gives the added advantage that it provides the desired low values of 'N_o' without increasing the drive in time and hence the diffusion length 'L_d' and also the characteristic length 'L'.

The etchant used was a solution of HF, HNO_3 and CH_3 COOH in ratio of 1:8:1 by volume. The etch rate of this solution was found to be 5.2 micron/min. Two phosphorous diffused samples (1 and 2)were etched in this solution for 25 sec. and 30 sec. respectively. For first case, the expected surface concentration was 1.03×10^{17} cm^{-3} and for the second it was 2×10^{16} cm^{-3}.

Diffusion Length(L_d): The diffusion length (L_d) is given as,

$$L_d = 2 \sqrt{D.t}$$

where, D = Diffusion co-efficient of the impurity atoms (cm.^{2}/sec.)
    t = Diffusion time (sec.)

This diffusion length,'L_d', is a parameter of Gaussian impurity distribution obtained from drive-in of impurities and is different from characteristic length, 'L', defined earlier in Chapter II and III, which is related with the exponential distribution, an approximation to the tail of the impurity distribution obtained by the diffusion process.

<u>Step IV</u>   Boron Diffusion:

Boron Nitride (BN) wafers were used as a solid state source for boron diffusion. Before the diffusion was carried out, the cleaned BN wafer was oxidised at $900^\circ C$ for 20 minutes with oxygen flow rate maintained at 200 c.c./min. The samples were then loaded for p-type diffusion. Since the junctions were required to be shallow p^+- n type, only deposition was carried out at $950^\circ C$ for 30 min. with nitrogen flow rate of 550 c.c./min. The expected junction depth and the measured sheet resistance were 0.26 micron and 9 ohms/ respectively. From these data the surface concentration was determined to be $4 \times 10^{20} cm^{-3}$ [28].

The shallow junction could also be obtained by carrying out deposition at high temperatures [$1000^\circ C$-$1200^\circ C$] for a less time duration . But it was observed that it gives rise to the formation of some compound of silicon and boron which is not possible to remove. Therefore, it was decided to carry out the deposition at lower temperature.

<u>Step V</u>   Ohmic Contacts:

The n surface i.e. the unpolished back side of the wafer, was lapped with 9 micron Al_2O_3 powder so as to remove the p-diffused layer completely. Ohmic contact, to this side, then , was made by electroless nickle plating [30]. The front side $\gamma(p^+$-side), being very heavily doped, is expected to provide a good ohmic contact to the metal probes.

Step VI   Mesa Etching:

A thick solution of apiezon wax (black wax) was made in tri-chloroethylene and the small dots of this solution were put on the p^+- side of the wafer with the help of a syringe. The unpolished side was completely covered with apiezon wax. Since the apiezon wax is not reacted upon by the etching solution, the etching of this masked wafer resulted in the mesa diodes of area nearly equal to the area of the dots on the polished side. The wax was then removed by dissolving it in tri-chloroethylene.

4.2   Measurements:

Out of a number of junctions fabricated , a small number was found to exhibit a sharp breakdown. The measurements were taken on three representative junctions (Jn. 1 on sample 1 and jn. to and 3 on sample 2) only. The breakdown voltages were measured directly from, the current - voltage characteristic displayed on the curve tracer.

The capacitance measurements were taken on a Boonton Electronics Corporation, type 74C-S18 capacitance bridge This is a fixed frequency (100 KC) bridge which reads an accuracy of 0.25 percent in absence of any shunt conductance. The respective voltages were measured on a 'Sensitive DC Meter, Model 95A,' manufactured by Boonton Electronics Corporation. The observed capacitances for the three junctions are plotted as a function of the voltage,
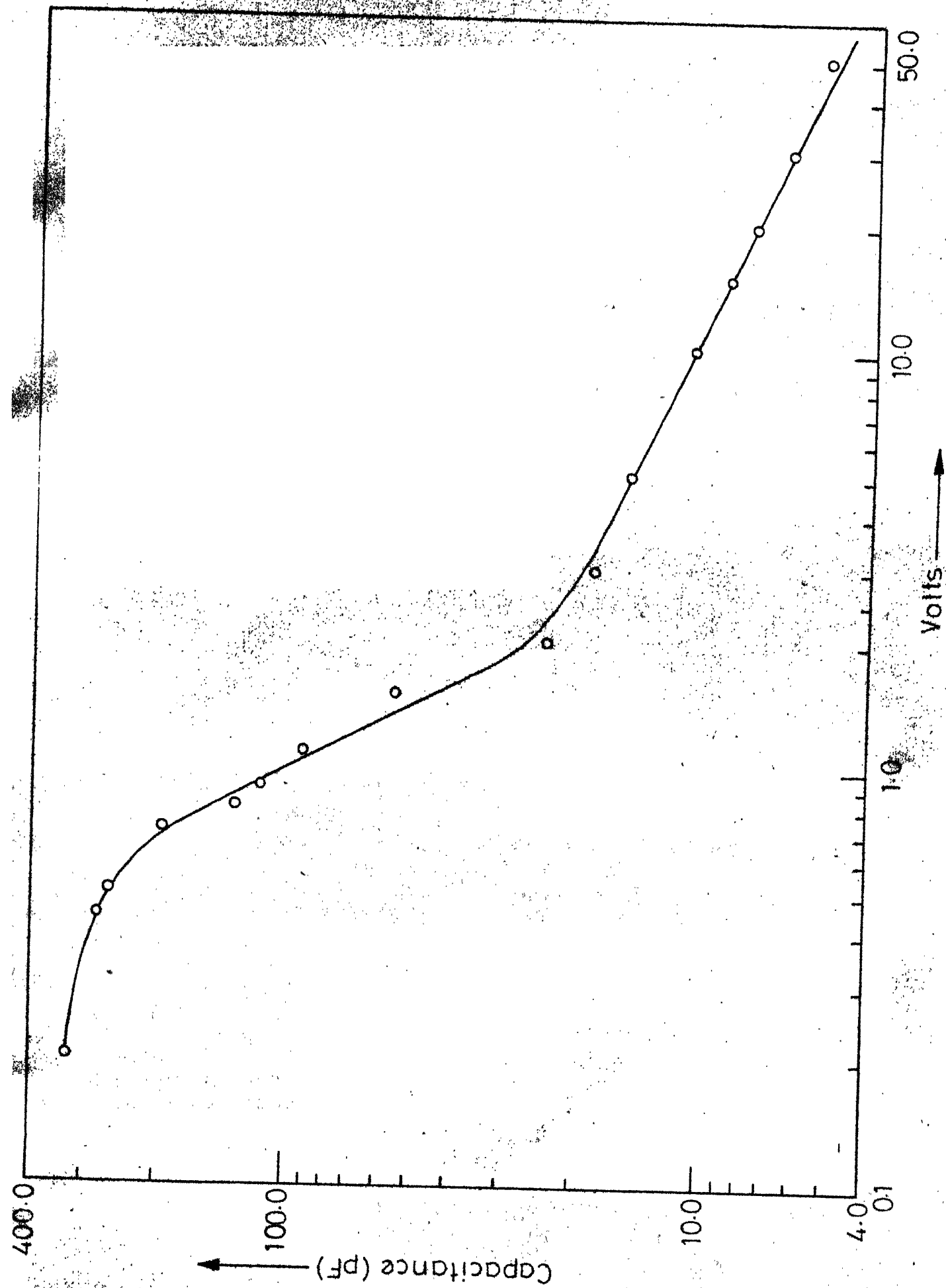
Fig.8(a) - C–V characteristic of JN. # 1.
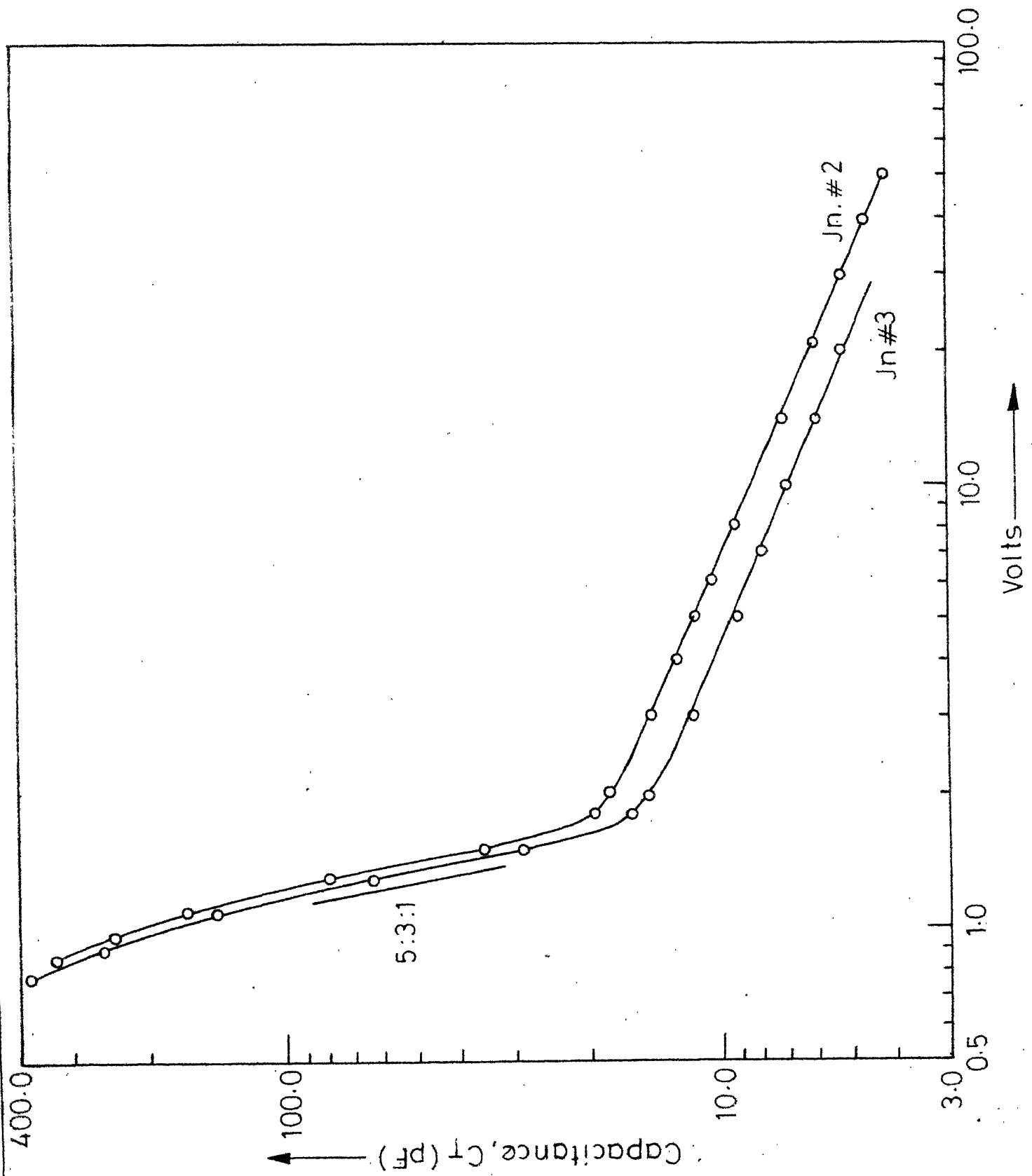
Fig.9(a)-C-V characteristics of JN.#2 and 3.

on log-log graph paper, in Fig. (8)a and Fig. (9)a.

4.3   Determination of Impurity Profile in Retrograded Region :

Impurity distribution in the retrograded region has been determined by the C-V characteristic of the junction. Assuming that (i) junction is one-sided (ii) all the impurity atoms near the junction are completely ionized, and (iii) all the voltage drop occurs in the space charge region, the impurity concentration at any point can be given, in terms of capacitance and voltage, by the following expressions [31],

$$N(x) = \frac{C_T^3}{A^2 . q . \varepsilon} . \frac{dV}{dC_T} \qquad (4.1)$$

and, $$x = \frac{\varepsilon . A}{C_T} \qquad (4.2)$$

where C_T = ~~Total~~ capacitance of the junction

A = Area of the diode

x = Distance from the junction.

N(x)= Impurity concentration at ~~the~~ distance 'x'
from the junction

V = Voltage across the junction.

The eq. (4.1) can also be written as,

$$N(x) = \frac{C_T^2}{A^2 . q . \varepsilon} . \frac{V}{n} \qquad (4.3)$$

where 'n' has its usual meaning.

The values of 'n' were measured at different points of C-V characteristics [Fig. (8)a and Fig. (9)a] and the values

Fig. 8(b).

Jn #1

x (micron) ⟶

$N(x), cm^{-3}$

Fig. 9(b).

Jn # 2 and 3

x (micron) ⟶

$N(x), cm^{-3}$
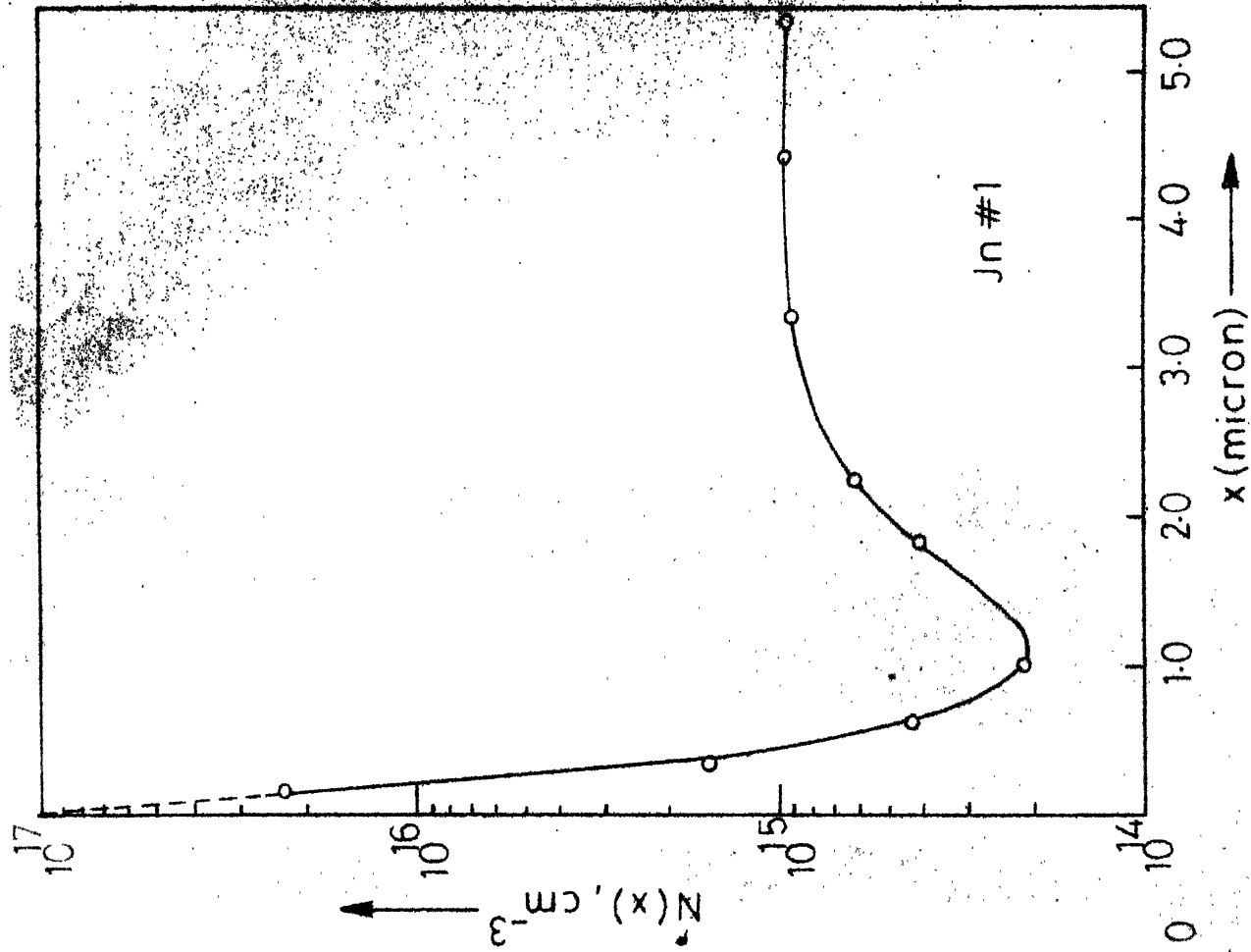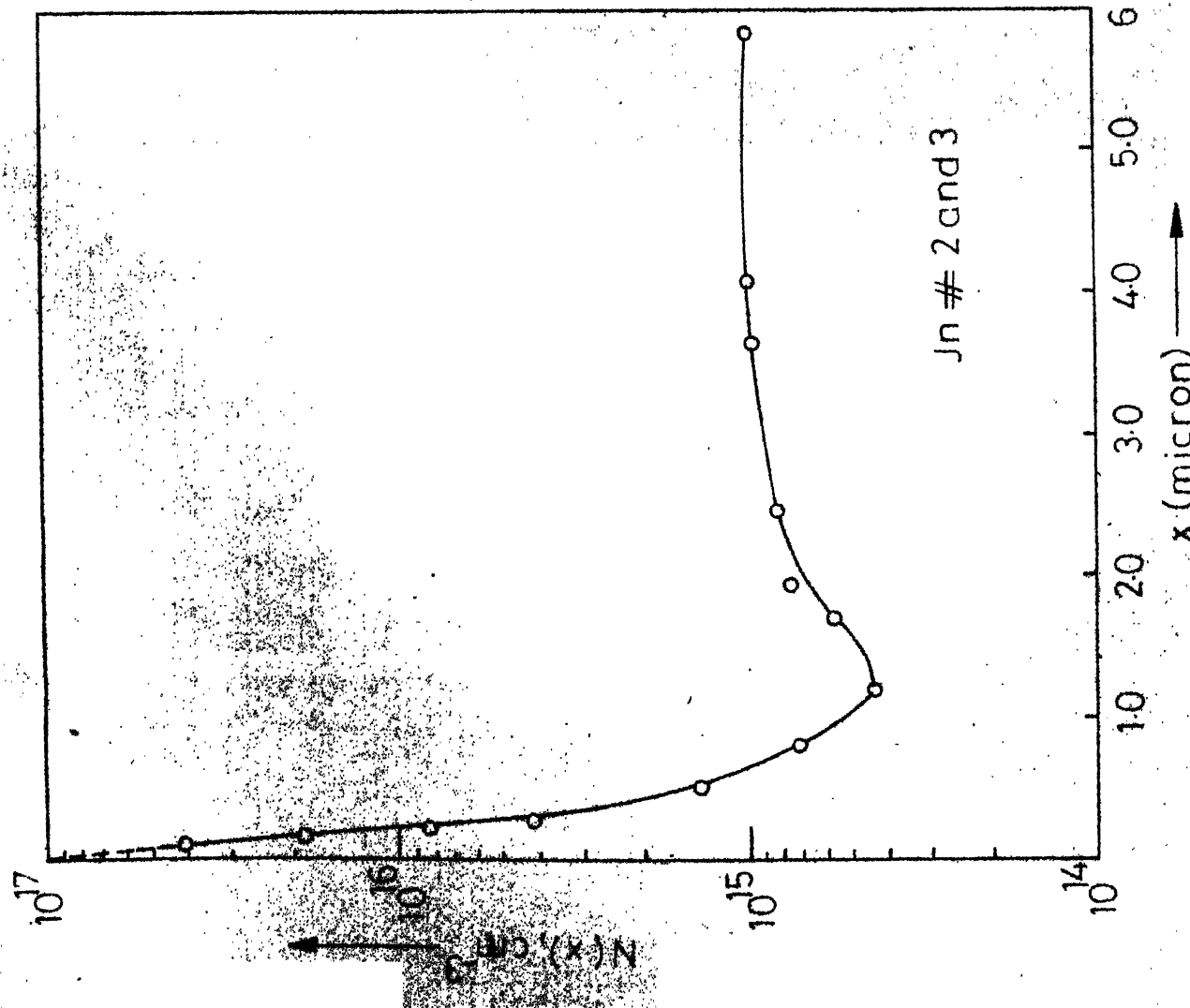
IMPURITY PROFILES.

of 'x' and 'N(x)' were calculated by using eqs. (4.2) and
(4.3) respectively. 'N(x)' has been plotted as a function
of 'x' (Fig. (8)b ,Fig. (9)b). The impurity profiles in
retrograded regions of junction   2 and   3 are same, as
expected.

4.4   Results and Discussion:

From the impurity profiles of retrograded region,
obtained from the C-V measurements of the junction, the
characteristic parameters of the impurity distribution
for various junctions have been determined. From Fig.
(8)b and Fig. (9)b it is seen that' $\ln[N(x)]$' versus 'x'
plot is linear near the junction, indicating that impurity
distribution is exponential in this region. The cross over
impurity concentration, 'N_0' has been determined by extra-
polating the straight line portion of the plot to x=0.
The values of 'N_0' for the junctions of sample # 2 is
observed to be lower than that for junction of sample # 1,
which is expected, for the sample   2 has been etched for
a longer time. The distance, in which   '(N_0-N_B)', which
is nearly equal to 'N_0' in these junctions, drops to ' 1/e'
of its initial value, gives the value of 'L' ... The substrate
impurity concentration is found to be 10^{15} cm^{-3}, which
corresponds to a substrate resistivity of 3.2 ohm.cm. This
value is in the range of resistivity specified by the
manufacturer (3-7 ohm cm.).

Both the impurity profiles, shown in Fig. (8)b and
Fig. (9)b, have a peculiar feature and that is, the dip in the
impurity profile, just preceding the region of constant
impurity concentration of substrate. No   plausible explai-
nation can be given at present for this unexpected result.

The 'V_B' and 'n_{max}' as measured for the various
junctions, along with the respective parameters characteriz-
ing the impurity distribution in retrograded region are
given in table 1. '$N_{min.}$', given in the table, is the
impurity concentration at the lowest point in the dip,
mentioned before.

Since the eq. (2.11), for 'V_B' does not hold
good for the values of 'L' below 0.3 micron, the value of
'V_B' could not be calculated for these junctions.
However, it is seen that the junctions with the lower 'N_o'
have a higher breakdown voltage, which is expected (see
Table 1).

The comparison of theoretically calculated '$n_{max.}$',
and measured values of '$n_{max.}$' (Table 1) brings out certain
interesting points. In case of junctions of sample   2 ,
the measured value of '$n_{max.}$', is in close agreement with the
calculated 'n_{max}' [using eq. (3.7)], if in the calculation of
'n_{max}', 'R_C' is taken to be equal to '$N_{min.}/N_o$. But the
calculated and measured values of '$n_{max.}$' come out to be
considerably different if 'R_C' is taken to be equal to

TABLE 1

Results of Measurements

	Jn.	N_0 (cm^{-3})	L (Micron)	N_B (cm^{-3})	$N_{min.}$ (cm^{-3})	V_B (Volts)	n_{max}	Area (cm^{-2})	Calculated results with N_0, L' and N_B as determined by expt. n max.		
									V_{13} (Volts)	with $R_C = \frac{N_B}{N_0}$	with $R_C = \frac{N_{min}}{N_0}$
Sample #1	Jn. #1	10^{17}	0.1	10^{15}	4.2×10^{14}	120	2	0.385×10^{-2}	—	2.3	4.2
Sample #2	Jn. #2	6×10^{16}	0.1	10^{15}	2.2×10^{14}	140	5.3	0.3×10^{-2}	—	2.0	4.8
	Jn. #3	6×10^{16}	0.1	10^{15}	2.2×10^{14}	138	5.3	0.25×10^{-2}	—	2.0	4.8

N_B/N_o. Exactly reverse is the case for the junction .
If '$n_{max.}$" is calculated with 'R_C' equal oto N_B/N_o, it gives
a value very close to the measured value of '$n_{max.}$' while
the agreement between calculated '$n_{max.}$' and measured $n_{max.}$
is very poor if 'R_C" is given a value equal to ' $N_{min.}/N_o$'.

CONCLUSION

Avalanche breakdown voltage for exponentially
retrograded silicon p-n junctions have been calculated for
various combination of parameters of exponential impurity
distribution. The empirical relationships [eq.(2.11) and
eq. (2.12)], expressing the breakdown voltage and space
charge width at breakdown as a function of the impurity
profile parameters, have been established. The calculated
results mark the upper bound of breakdown voltage. In
actual junctions, the breakdown voltage is expected to be
less than this bound because of microplasmas and the
junction curvature.

The calculated breakdown voltages have been compared
with those reported by M.Shinoda [5]. It has been observed
that for the same impurity profiles, the breakdown voltages
reported by M.Shinoda are higher. However, our results for
breakdown voltages are expected to be in better agreement with
the experimental results than those reported by M.Shinoda.,
for the reason that more accurate values of ionization rates for
for holes and electrons have been used for calculation of
breakdown voltage.

The dependence of C-V index on the impurity profile
parameter has also been studied. It is observed that nearly
in all the cases considered, the junction shows up its
hyperabrupt nature only in the range, $0.1cm \leq C \leq 10cm$

[Fig.(5)] where $'C_m'$ is the value of normalized capacitance at $n = n_{max}$ Outside this range of $'C'$, the junction approaches an abrupt junction . Moreover the peaks of the curves in Fig. (5) can be said to be the most important points because these are the points which make the hyperabrupt junction superior to the other types of junctions. Also it is only at these points that $'n'$ (which is equal to n_{max}. at the peak) remains constant over a small range of voltages [Fig. (7)], which is a requirement in most of the applications of varactors. The empirical relationships,relating $'n_{max}$.$'$, $'C_m'$ and R_c, have been obtained [eqs. (3.6) and (3.7)] by using linear regrassion technique.

The four equations [(2.11),(2.12), (3.6) and (3.7)] form a part of the set of design equations for silicon hyperabrupt junctions. In the design of varactors, two different types of situations can be encountered. First is where the range of variation of capacitance is of primary interest and second where the value of $'n'$ is the main criterian of design. The starting point of the design in both these situations, is the assumption of an impurity profile ,based on the requirements of cut off frequency of the varactor. For a given impurity profile, the above empirical equations may be used/in the design of varactors   as explained below.

Considering the first type of situations, the minimum capacitance corresponds to the space charge width $'W_B'$ can be determined by substituting $'N_o'$, $'L'$ and $'N_B'$ in equation (2.12). The corresponding voltage can be calculated by Eq. (2.11). For the calculation of maximum available capacitance none of the four equations is helpful. It can however, be determined by using Lawrence and Warner's plots [32].

For the second type of situation where C-V index (n) is the design criterian, $'n_{max}'$ is calculated first by eq. (3.7). For this value of $'n_{max}'$, $'C_m'$ and hence $'W_m'$ ($= \frac{L}{C_m}$) is then determined by eq. (3.6). $'W_B'$ is now, calculated by substituting $'N_o'$, $'L'$ and $'N_B'$ in eq. (2.12). Since in most of the applications, it is desired that the junction is operated at $n = n_{max}$, the $'W_m'$ should be smaller than $'W_B'$. By the iteration of this calculation procedure, a compromise between cut-off frequency, which is partly determined by $'N_o'$, $'L'$ and $'N_B'$, and $'n_{max}'$, can be reached.

In an attempt to verify some of the results of our calculations, hyperabrupt junctions were fabricated by double diffusion technique . The main problem encountered in the fabrication, was that of controlling the cross over concentration , $'N_o'$. The surface concentrations of impurities obtained by phosphorous diffusion were not in the acceptable range of $'No'$. So the surface concentration

was reduced by etching out a small thickness of wafers,
thus, exposing the surface of lower impurity concentration.
For a given etching rate, the 'N_0', thus could be controlled
by controlling the etching time only. The etchant used
for the purpose is felt to be having rather a high etching
rate, resulting in a some what poor control over 'N_0'. An
attempt to decrease the etching rate of this solution by
increasing the moderator (CH_3COOH) content ~~contained~~ was made.
No marked decrease in etching rate was observed, even when
the composition of etchant was changed from 1 part HF + 8
parts HNO_3 + 1 part CH_3COOH to 1 part HF + 8 parts HNO_3+ 3
parts CH_3COOH. Further increase in CH_3COOH content was
found to give rise to a thin whitish hazy deposition on the
surface. For the improvement in control of 'N_0' , it is
essential that an etchant of much lower etching rate, than
that used in the fabrication, is developed. For mesa
etching, the photolithography should certainly have given
better results as it gives the diodes of well defined
geometry,thus making it possible to measure the area of
the junction accurately. The evaporated gold dots probably
can also be used as a replacement to blackwax dots, which
were used for the mesa etching in the fabrication of hyper-
abrupt junctions.

The theoritical results could not be verified
experimentally. The experimental results, obtained from
the measurements on a few hyperabrupt junctions fabricated,

are rather inconsistent with the theoretical results.
However, because of the limited number of observations it is
not possible to draw any definite conclusions.

APPENDIX

The method of regression analysis consists of postulating a relationship between a dependent variable and independent variables and then determining the co-efficients of the independent variables, for the least sum of squares of residuals [residual is defined as the defference in the observed and estimated value of dependent variable]. The quantities 'R^2' and '$\bar{R}^2$' help in assessing the goodness of the equation in estimating the value of dependent variable for a given set of values of independent variables.

(i) R^2 : R^2 is given by

$$R^2 = 1 - \frac{e^2}{(Y-\bar{Y})^2}$$

where Y = observed values of dependent variable

$\bar{Y}$ = mean value of dependent variable

e^2 = sum of square of residuals.

It is obvious from the expression for 'R^2' that the value of 'R^2' approaches unity when the value of residuals, 'e' approaches zero, i.e. when the value of dependent variable estimated by the equation, approaches the corresponding observed value of dependent variable for each observation.

(ii) $\bar{R}^2$: This is given by the relation,

$$\bar{R}^2 = 1 - \frac{V(e)}{V(Y)}$$

where

$$V(e) = \text{Variance of residual} = \frac{e^2}{n_f}$$

$$V(Y) = \text{Variance of dependent variable}$$

$$= (Y-\bar{Y})^2/(n-1)$$

n_f = Degrees of freedom

K = Total number of co-efficients including constant term

n = Total number of observations.

With the addition of variables /terms to the equation, 'R^2' necessarily increases regardless of the relevance or otherwise of the indluded term. This is because of decline in ' e^2 '. Here in, the value of 'R^2' assumes importance. For the degrees of freedom also decreases and hence '$V(e)$' may become less or more, depending upon the relative reduction in ' e^2 ' and 'n_f' . Thus , if the addition of a term increases $\bar{R}^2$ also, it implies that after the inclusion of term, the expression has a better power of prediction due to the lessening of the variance of the error of prediction.

: REFERENCES:

1.   T.Terada,'Germanium Hyperabrupt Varactors',Electronics
      and Commn. in Japan, 49, n3,pp 3 (1966).

2.   T.Terada,'Reverse Characteristic of Germanium Hyperabrupt
      p-n Junctions', Electronics and Commn. in Japan, 52,
      n 1, pp 103 (1964).

3.   M.Kobayashi, et.al.,'Breakdown Voltage of Germanium
      Hyperabrupt Junctions', Electronics and Commn. in
      Japan, 52, n 9, pp 167 (1969).

4.   Nathanson et.al.,"On Multiplication and Avalanche
      Breakdown in Exponentially Retrograded Silicon p-n
      Junctions,' IRE Trans. on Electron Devices, ED-10,
      pp 44 (1963).

5.   M.Shinoda, 'Avalanche Breakdown of Hyperabrupt Junctions'
      Electronics and Commn. in Japan 52, n 4,pp 15 (1969).

6.   K.G.Mckay, 'Avalanche Breakdown in Silicon', Phy. Rev.
      Vol. 94, pp 877, May (1954).

7.   Y.Watenbe, 'Semiconductors and Transistors', Ohms book
      Co. (1959).

8.   C.A.Lee et.al.,'Ionization Rates of Holes and Electronics
      in Silicon', Phy. Rev., Vol. 134A, pp 761 (1964).

9.   A.G.Chynowith, 'Uniform Silicon p-n junctions,II.
      Ionization Rates for Electrons', J.App.Phy.,31,pp 1161
      (1960).

10. A.G.Chynowith,'Ionization Rates for Holes and Electrons In Silicon', Phy. Rev., 109, pp 1537. (1958).

11. S.L.Miller, 'Ionization Rates for Holes and Electrons in Silicon ', Phy. Rev., 105, pp 1246 (1957).

12. J.L.Moll and R.Van Overstraeten, Solid State Electronics, 6, pp 147 (1963).

13. R.Van Overstraeten, H.D.Man, 'Measurement of Ionization Rates in Diffused Silicon p-n Junctions', Solid State Electronics ,13, pp 583 (1970).

14. M.H.Wood et.al.,' Use of Schottky Barrier to Measure Impact Ionization Coefficients in Semiconductors',Solid State Electronics,16 ,pp 381 (1973).

15. R.M.Warner, 'Avalanche Breakdown in Silicon Diffused Junctions', Solid State Electronics, 15,pp 1303 (1972).

16. A.Shimiju et.al., 'Alloy Diffused Variable Capacitance Diode with Large Figure of Merit', IRE Trans. on Electron Devices, ED-8, pp 370 (1961).

17. M.Shinoda, 'Capacitance of Hyperabrupt Junction Fabricated by Alloy Diffusion Technique', Electronics and Comm. in Japan, 47, n3, pp 66 (1964)

18. Norwood M.H.and Shatz E., 'Voltage Variable Capacitor Tuning , A Review ', Proc. IEEE, 56, pp 788 (1968)

19. Sukegawa et.al., 'A Design Method For Variable Capacitance Diodes with mth Power Characteristic for a Wide Range of Voltage', IEEE Trans. on Electron Devices, ED-13, pp 988 (1966).

20. Sze and Gibbons, 'Avalanche Breakdown Voltage of Abrupt and Linearly Graded p-n junctions in Ge, Si, GaAs and Ga P.', App. Phy. Letters, 8, pp 111 (1966).

21. M.S.Tyagi, 'Zener and Avalanche Breakdown in Silicon Alloyed p-n Junctions-I, Analysis of Reverse Characteristic Solid State Electronics, 11, pp 99 (1968).

22. Rao and Miller, 'Applied Econometrics', Prentice Hall (1972).

23. Thomas and Boothroyd, 'Physical Model for Double Diffused Transistors! Solid State Electronics, 11, pp 365 (1968).

24. Kannam et.al., 'Design Considerations for Hyperabrupt Varactors', IEEE Trans. on Electron Devices, ED-18, pp 109 (1972).

25. Nakanuma, S., 'Silicon Variable Capacitance Diode with High Voltage Sensitivity by Low Temperature Epitaxial Growth', IEEE Trans. on Electron Devices, ED-13, pp 578 (1966).

26. R.A.Moline and G.F.Foxhall, 'Ion Implanted Hyperabrupt Junction Voltage Variable Capacitors', IEEE Trans. On Electron Devices, ED-19, pp 267 (1972).

27. Sze and Gibbons, 'Effect of Junction Curvature on Breakdown Voltage in Semi Conductors, 'Solid State Electronics, 9, pp 831 (1966).

28. H.C.Lin, 'Integrated Electronics', pp 148, Holden-day Series in Information Systems.

29. R.A.Sunshine and J.Assour,' Avalanche Breakdown Voltage of Multiple Epitaxial p-n Junctions', Solid State Electronics, 16, pp 459 (1973).

30. Sullivan M.V. and Eigler J.H.,'Electroless Nickle Plating for Making constant to Silicon',J.Electrochem. Soc.,104, pp 226 (1957).

31. Hillbrand and Gold,'Determination of Impurity Distribution by C-V Measurements', RCA Rev., pp 245 (1960).

32. H.Lawrence and R.M.Warner, Jr,,'Diffusion Junction Depletion Layer Calculations, 'Bell Sys.Tech.Jour., 39, pp 389,March (1960)